

Silencing of long non-coding RNA LINC00958 inhibits head and neck squamous cell carcinoma progression and AKT/mTOR signaling pathway by targeting miR-106a-5p

Y.-F. YANG^{1,2}, L. FENG^{1,2}, Q. SHI², L.-W. WANG^{1,2}, L.-Z. HOU^{1,2}, R. WANG^{1,2}, J.-G. FANG¹⁻³

¹Department of Otolaryngology Head and Neck Surgery, Beijing Tongren Hospital, Capital Medical University, Beijing, China

²Key Laboratory of Otolaryngology Head and Neck Surgery (Ministry of Education of China), Beijing Institute of Otolaryngology, Beijing, China

³Beijing Key Laboratory of Head and Neck Molecular Diagnostic Pathology, Beijing, China

Abstract. – OBJECTIVE: The long non-coding RNA LINC00958 acts as an oncogenic regulator in many human tumors. In this study, we aimed to investigate the role and potential molecular biological mechanisms of LINC00958 in head and neck squamous cell carcinoma (HNSCC).

MATERIALS AND METHODS: Aberrantly expressed LINC00958 was screened out of TC-GA database. The quantitative Real Time-Polymerase Chain Reaction (qRT-PCR) was used to determine LINC00958 and miR-106a-5p expression. Cellular biological behaviors were investigated using CCK-8, colony formation, wound healing and transwell assays. Xenograft mouse models were established to determine the role of LINC00958 in HNSCC growth *in vivo*. The interaction between LINC00958 and miR-106a-5p was validated by Dual-Luciferase reporter gene assay. Additionally, the underlying pathways affected by LINC00958 were measured by Western blot.

RESULTS: LINC00958 expression was up-regulated in HNSCC tissues and cells. High LINC00958 level was correlated with the poor prognosis of HNSCC patients. Functional assays showed that the knockdown of LINC00958 inhibited HNSCC malignant phenotypes *in vitro* and *in vivo*. Mechanistically, miR-106a-5p was a potential target of LINC00958, and its expression was negatively regulated by LINC00958 in HNSCC. LINC00958 could activate AKT/mTOR signaling pathway, which was mediated by miR-106a-5p.

CONCLUSIONS: Taken together, our results suggest that LINC00958 acts as an oncogenic role in HNSCC and activates AKT/mTOR signaling pathway by sponging miR-106a-5p. LINC00958 may serve as a potential target for HNSCC diagnosis and treatment.

Key Words:

Head and neck squamous cell carcinoma, Long non-coding RNA LINC00958, MiR-106a-5p, AKT/mTOR signaling pathway.

Introduction

Head and neck squamous cell carcinoma (HNSCC) is the sixth most common malignancy, affecting approximately 600,000 people annually. Despite advances in screening, diagnosis and comprehensive therapy, about 40-50% of HNSCC patients die from their disease¹. HNSCC encompasses a group of cancers that arise in the squamous mucosal surfaces of the upper aerodigestive tract, including the oral cavity, pharynx, and larynx². Multiple molecular changes are required to drive the malignant progression of HNSCC¹. Thus, elucidating the molecular mechanisms of HNSCC carcinogenesis and determining novel molecular targets are essential to develop effective therapeutic strategies for HNSCC.

Long non-coding RNAs (lncRNAs), a class of non-protein coding transcripts over 200 nucleotides in length, are engaged in diverse biological processes of human cancers³. The aberrantly expressed lncRNAs might serve as treatment target and diagnostic biomarkers for various cancers, including HNSCC⁴. Long non-coding RNA 00958 (LINC00958) is originally identified as an oncogene in bladder cancer⁵. LINC00958 involves in the biological process of several other malignancies via

sponging microRNA (miRNA). Competing endogenous RNA (ceRNA) forms a large-scale regulatory network across the transcriptome, playing important roles in cancer⁶. LINC00958 could serve as a ceRNA, for example, in hepatocellular carcinoma and aggravates malignant phenotypes by serving as a sponge for miR-3619-5p⁷. In cervical cancer, LINC00958 regulates cell sensitivity to radiotherapy by binding to miR-5095⁸. In lung adenocarcinoma, LINC00958 facilitates cell proliferation, migration and invasion *via* mediating miR-625-5p⁹. In pancreatic cancer, silencing of LINC00958 prevents tumor initiation by acting as a sponge of miR-330-5p¹⁰. However, the regulatory network of LINC00958 *via* sponging miRNA in the tumorigenesis and progression of HNSCC has not yet been documented, thus needs further explorations.

In the current study, we found that LINC00958 was significantly upregulated in HNSCC tissues and cell lines. Moreover, high level of LINC00958 was associated with poor survival outcomes of HNSCC patients. Functional assays showed that LINC00958 knockdown inhibited HNSCC malignant phenotypes *in vitro* and *in vivo*. Mechanistically, we firstly found that LINC00958 could regulate the AKT/mTOR signaling pathway and the progression of HNSCC by acting as a sponge of miR-106a-5p. Taken together, LINC00958 could be a good candidate for HNSCC prognosis and therapy.

Materials and Methods

Bioinformatics Analysis

The Cancer Genome Atlas (TCGA) (<https://portal.gdc.cancer.gov/>) and Gene Expression Profiling Interactive Analysis (GEPIA) (<http://gepia.cancer-pku.cn>) was used to obtain LINC00958 expression in HNSCC tissues and adjacent normal tissues. The prognosis analysis of HNSCC patients was calculated using the Kaplan-Meier method by GEPIA. The RNA22 database (<http://cm.jefferson.edu/rna22/>) was used to predict miRNA that combined with lncRNA. The StarBase database (<http://starbase.sysu.edu.cn/>) was used to reveal the correlation between the expression of miRNA and lncRNA in HNSCC tissues.

Cell Lines and Cell Culture

Human HNSCC cell lines (FaDu, Cal-27, SCC4, and SCC9) and human immortalized keratinocytes cell line (HaCaT) were brought from American Type Culture Collection (ATCC; Manassas, VA, USA). The FaDu and Cal-27 cells

were cultured in Dulbecco's Modified Eagle's Medium (DMEM; Gibco, Grand Island, NY, USA). SCC4 and SCC9 cells were cultured in DMEM/F12 (Gibco, Grand Island, NY, USA). HaCaT cells were cultured in Roswell Park Memorial Institute (RPMI-1640; Gibco, Grand Island, NY, USA). All the medium was supplemented with 10% fetal bovine serum (FBS; Gibco, Grand Island, NY, USA), and 1% penicillin/streptomycin (Beyotime Biotechnology, Pudong, Shanghai, China). Cell mediums were maintained in an incubator containing 5% CO₂ at 37°C. All cells tested negative for mycoplasma contamination, and this result was authenticated by short tandem repeat (STR) fingerprinting before use.

Cell Transfection

Recombinant lentivirus for LINC00958 knockdown and its negative control (NC) were designed and obtained from Taitool Bioscience (Jiading, Shanghai, China). The target sequences for LINC00958 small short hairpin RNAs (shRNAs) were showed as follows: 5'-GTACCCAAGTTATTCAGGATT-3' (sh-LINC00958-#1), 5'-GTGACTAGCTTAAACTA-AATT-3' (sh-LINC00958-#2), and 5'-GAGGTAC-CCAATAGTTTCATT-3' (sh-LINC00958-#3). Lentiviruses were transfected into HNSCC cells for 48 h. The knockdown efficiency was detected by quantitative Real Time-PCR reactions (qRT-PCR). Moreover, miR-106a-5p inhibitor, and corresponding NC (miR-NC) obtained from RiboBio Company (Guangzhou, Guangdong, China) were used to generate knockdown-miR-106a-5p model.

RNA Extraction and Quantitative Analysis

Total RNA was extracted from HNSCC samples and cell lines by TRIzol reagent (Invitrogen, Carlsbad, CA, USA). Reverse transcription was performed using a Transcriptor First Strand cDNA Synthesis Kit (Roche, Basel, Switzerland) and a TaqMan miRNA reverse transcript kit (Applied Biosystems, Branchburg, NJ, USA). An ABI PRISM 7500 sequence detection system (Applied Biosystems, Foster City, CA, USA) was employed to conduct quantitative Real Time-PCR reactions (qRT-PCR). The expression of LINC00958 was normalized to housekeeping gene glyceraldehyde-3-phosphate dehydrogenase (GAPDH), while the expression of miR-106a-5p was normalized to the housekeeping gene U6. The gene expression fold changes were calculated based on the 2^{-ΔΔCt} method. Each test was repeated three

times. Specific primer sequences were as follows: LINC00958 forward: 5'-CCATTGAAGA-TACCACGCTGC-3'; LINC00958 reverse: 5'-GGTTGTTGCCAGGGTAGTG-3'; GAPDH forward: 5'-GATCATCAGCAATGCCTCCT-3'; GAPDH reverse: 5'-TGAGTCCTTCCACGATAC-CA-3'; miR-106a-5p forward: 5'-GCGAAAAGT-GCTTACAGTGCAGGTAG-3'; miR-106a-5p reverse: 5'-GTGCAGGGTCCGAGGT-3'; U6 forward: 5'-CTCGCTTCGGCAGCACA-3'; U6 reverse: 5'-AACGCTTCACGAATTTGCGT-3'.

Cell Proliferation Assay

For Cell Count Kit-8 (CCK-8) assay, the HNSCC cells were plated in 96-well plates (2000 cells/well). Cell proliferation was determined every 24 h for 4 days according to the manufacturer's instruction. Briefly, 10 μ L of CCK-8 solution (MedChemExpress, Pudong, Shanghai, China) was added to each well. After incubation at 37°C for 1 h, the absorbance at 450 nm was measured using microplate reader (Multiscan FC, Thermo Scientific, Waltham, MA, USA). The experiments were repeated three times and six parallel samples were measured each time. For colony formation assay, 1000 HNSCC cells were seeded into each well of a 6-well plate and maintained in a medium containing 10% FBS for 14 days. The colonies were fixed with 1% formaldehyde solution and stained with 0.1% crystal violet. Photos of colonies were taken by camera and number of colonies was calculated by Image J software. The experiment was repeated three times.

Cell Migration and Invasion Assays

For wound healing assays, HNSCC cells were grown to near confluence in six-well plates and then subjected to serum-free medium for 24 h. Artificial wounds were scratched on the monolayer, and images were captured at 0 h and 48 h. Transwell migration and invasion assays were performed using transwell chambers (8- μ m pores, Corning, NY, USA) that coated without or with Matrigel (BD, Biosciences, NJ, USA). HNSCC cells (5×10^4) suspended in serum-free medium were plated in the upper chambers. Medium supplemented with 10% FBS was placed in the lower chambers. After incubation for 18 or 24 h, the migrated or invaded cells were fixed with 1% formaldehyde solution, stained with 0.1% crystal violet, and captured under a light microscope (Olympus, Tokyo, Japan). The cell numbers were counted in five random fields.

Dual-Luciferase Reporter Gene Assay

Potential targeted miRNAs of LINC00958 were identified on RNA22 database (<http://cm.jefferson.edu/rna22/>). The Luciferase reporter plasmids (pGL3) containing LINC00958 wild type (WT) or LINC00958 mutant type (MUT) were constructed, and co-transfected with miR-106a-5p mimic or NC mimic into HNSCC cells. Cell transfection was performed using Lipofectamine 3000 (Invitrogen, Thermo Fisher Scientific, Waltham, MA, USA). 48 h later, firefly and *Renilla* luciferase activity was examined by the Dual-Luciferase Reporter Assay System (Promega, Madison, WI, USA), and *Renilla* activity was used to normalize firefly activity.

Western Blotting

Total proteins were extracted by using RIPA (Applygen, Changping, Beijing, China). A BCA Protein Assay Kit (Beyotime, Pudong, Shanghai, China) was used to quantify the concentration of protein. Protein samples were electrophoretically separated by SDS-PAGE and transferred to a Polyvinylidene difluoride (PVDF) membrane (Millipore, MA, USA). After blocking with 5% bovine serum albumin, the membranes were then incubated with the following primary antibodies: rabbit anti-human antibodies to GAPDH (Cell Signaling Technology, Danvers, MA, USA), AKT (Abcam, Cambridge, MA, USA), p-AKT (Abcam, Cambridge, MA, USA), mTOR (Abcam, Cambridge, MA, USA), p-mTOR (Abcam, Cambridge, MA, USA) at 4°C overnight. On the following day, the membrane was incubated with goat anti-rabbit antibody to IgG (Beyotime, Pudong, Shanghai, China) for 1 h. Then, the protein strips were visualized and detected using an enhanced chemiluminescent reagent kit (Thermo Fisher Scientific, Waltham, MA, USA). Images were acquired by a ChemiDoc MP Imaging System (Bio-Rad, Hercules, CA, USA) and analyzed by the ImageJ software. GAPDH was used as an internal control.

Xenograft Tumor Assay

All of the animal experiments were performed according to guidelines approved by the Institutional Animal Care and Use Ethics Committee of the Capital Medical University. For the subcutaneous model, SCC4 cells (5×10^6) with LINC00958 knockdown, and the corresponding controls (stably transduced with sh-NC lentivirus) were injected subcutaneously into nude mice. All mice were sacrificed 30 days after injection, and tumors from each animal were weighed.

Statistical Analysis

SPSS 22.0 software (SPSS Corp., Armonk, NY, USA) was used for data analysis. The differences between the normally distributed values of two experimental groups were analyzed by a paired *t*-test or unpaired *t*-test. Data among multiple groups were analyzed by one way analysis of variance (ANOVA) with Tukey's post hoc test. Overall survival (OS) was calculated using the Kaplan-Meier method, and the results of the analysis were considered significance in a log-rank test if $p < 0.05$. The data are expressed as mean \pm standard deviation (SD). The differences were considered significant if $p < 0.05$. * $p < 0.05$; ** $p < 0.01$; *** $p < 0.001$.

Results

LINC00958 Expression Was Upregulated and Associated With Poor Prognosis of HNSCC Patients

We initially analyzed the GEPIA database and found that LINC00958 expression was significantly higher in HNSCC tissues compared with that of adjacent normal tissues. (Figure 1A; $p < 0.05$). Meanwhile, primary HNSCC cell lines (FaDu, Cal-27, SCC4, and SCC9) expressed higher LINC00958 levels compared with human immortalized keratinocytes cell line (HaCaT, normal control; Figure 1B; p all < 0.05). Furthermore, the HNSCC patients with high LINC00958 expression showed poor overall survival rate compared with low LINC00958 expression (Figure 1C; $p = 0.0062$).

LINC00958 Knockdown Inhibited Malignant Behaviors of HNSCC *in vitro* and *in vivo*

To explore the biological function of LINC00958 on HNSCC cells, we knockdown LINC00958 using shRNAs (sh-LINC00958-#1, sh-LINC00958-#2, sh-LINC00958-#3, and a normal control sh-NC) in two HNSCC cell lines highly expressing LINC00958 (FaDu and SCC4). The efficiency was then determined by qRT-PCR. Sh-LINC00958-#1 and sh-LINC00958-#2 were selected for the following experiments as their better knockdown efficiencies (Figure 2A; p all < 0.01). The CCK-8 assay showed that down-regulation of LINC00958 significantly attenuated cell proliferation of FaDu and SCC4 cells (Figure 2B; p all < 0.001). This result was also confirmed by the colony formation assay (Figure 2C; p all < 0.01). Moreover, wound healing assay, transwell migration and invasion assays indicated that suppression of LINC00958 expression decreased the migratory and invasive abilities of FaDu and SCC4 cells (Figure 2D-F; p all < 0.001).

To further investigate whether low LINC00958 expression would suppress the growth of HNSCC tumors *in vivo*, we injected SCC4 cells with or without LINC00958 knockdown (sh-LINC00958-#2, and sh-NC) into the BALB/c nude mice. As indicated in Figure 2G, we found that LINC00958 knockdown resulted in a blunted tumor growth in terms of tumor weight ($p < 0.01$). Collectively, knockdown of LINC00958 inhibited the malignant behaviors of HNSCC *in vitro* and *in vivo*.

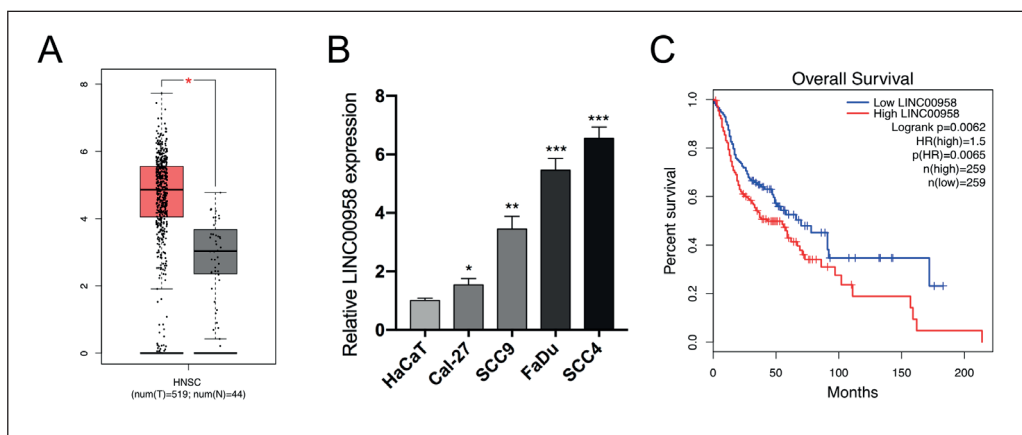
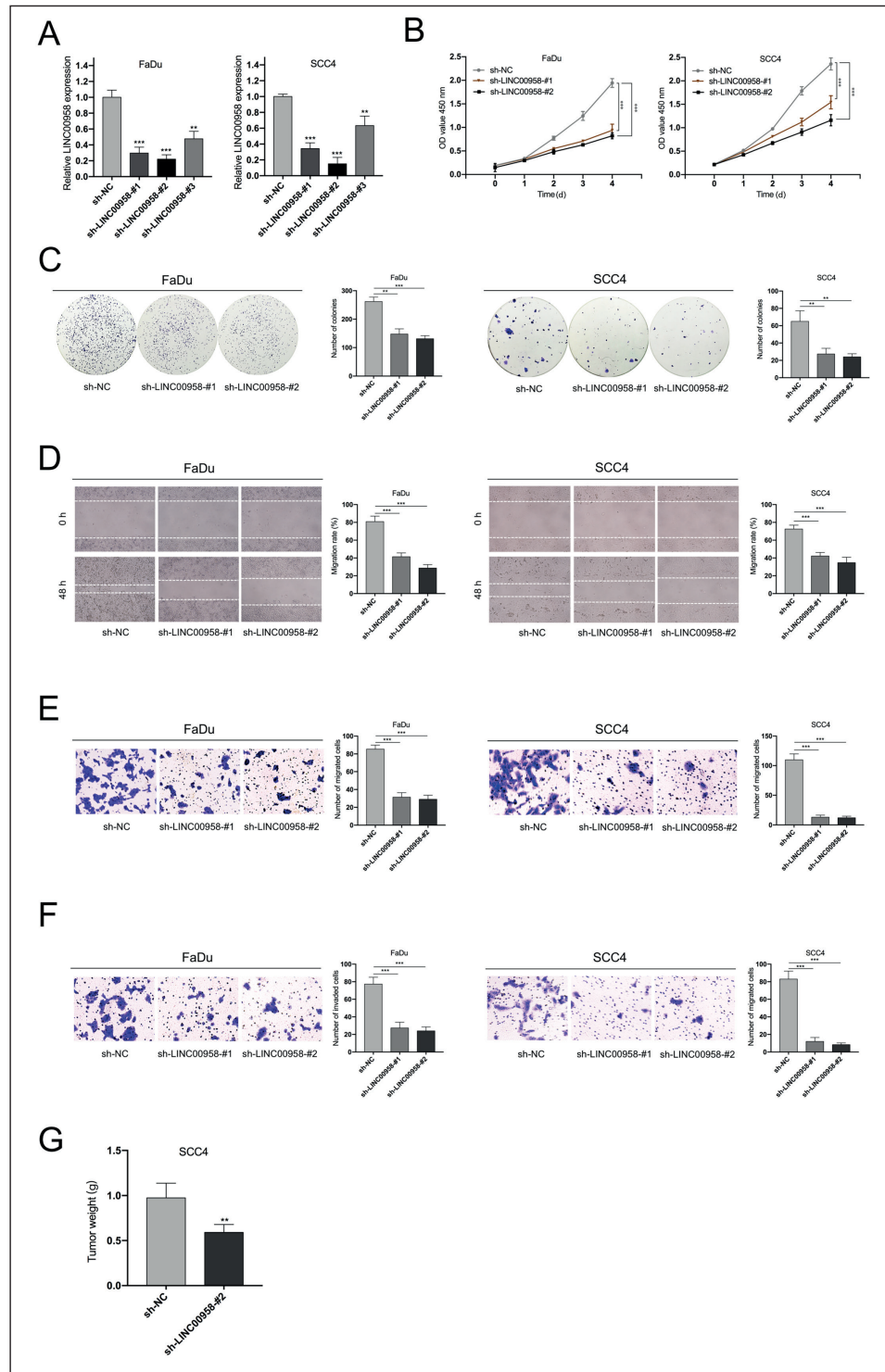


Figure 1. LINC00958 expression was upregulated and associated with poor prognosis of HNSCC patients. **A**, GEPIA database showed the upregulation of LINC00958 in HNSCC tissues compared with paired adjacent normal tissues. **B**, qRT-PCR analyses confirmed the upregulation of LINC00958 in HNSCC cells (FaDu, Cal-27, SCC4, and SCC9) compared with human immortalized keratinocytes cell line (HaCaT, normal control). **C**, GEPIA database showed that the upregulation of LINC00958 was correlated to poor prognosis of HNSCC patients. * $p < 0.05$, ** $p < 0.01$, *** $p < 0.001$ compared to the control group.

Figure 2. LINC00958 knockdown inhibited malignant behaviors of HNSCC *in vitro* and *in vivo*. **A**, The knockdown efficiency of LINC00958 in FaDu and SCC4 cells were analyzed by qRT-PCR. **B**, CCK-8 assays assessed the effects of LINC00958 knockdown on FaDu and SCC4 cell proliferation. **C**, Colony formation assays assessed the effects of LINC00958 knockdown on FaDu and SCC4 cell proliferation (magnification: 1×). **D**, Wound healing assays examined the effects of LINC00958 knockdown on FaDu and SCC4 cell migration (magnification: 20×). **E**, Transwell migration assays examined the effects of LINC00958 knockdown on FaDu and SCC4 cell migration (magnification: 100×). **F**, Transwell invasion assays evaluated the effects of LINC00958 knockdown on FaDu and SCC4 cell invasion (magnification: 100×). **G**, Curve of tumor weight in nude mice were plotted to indicate the effects of LINC00958 knockdown on SCC4 cell *in vivo*. ** $p < 0.01$, *** $p < 0.001$ compared to the control group.



LINC00958 Acted as a Sponge of MiR-106a-5p in HNSCC Cells

To explore the underlying regulatory mechanism of LINC00958, we used RNA 22 database and found that the 3'-UTR of LINC00958 possessed complementary sequences of miR-106a-5p (Figure

3A). Then, dual-luciferase reporter assay was performed to verify whether miR-106a-5p was a potential target of LINC00958 in HNSCC cells. The results displayed in Figure 3B suggested that FaDu and SCC4 cells co-transfected by LINC00958 WT and miR-106a-5p mimic exhibited significantly low

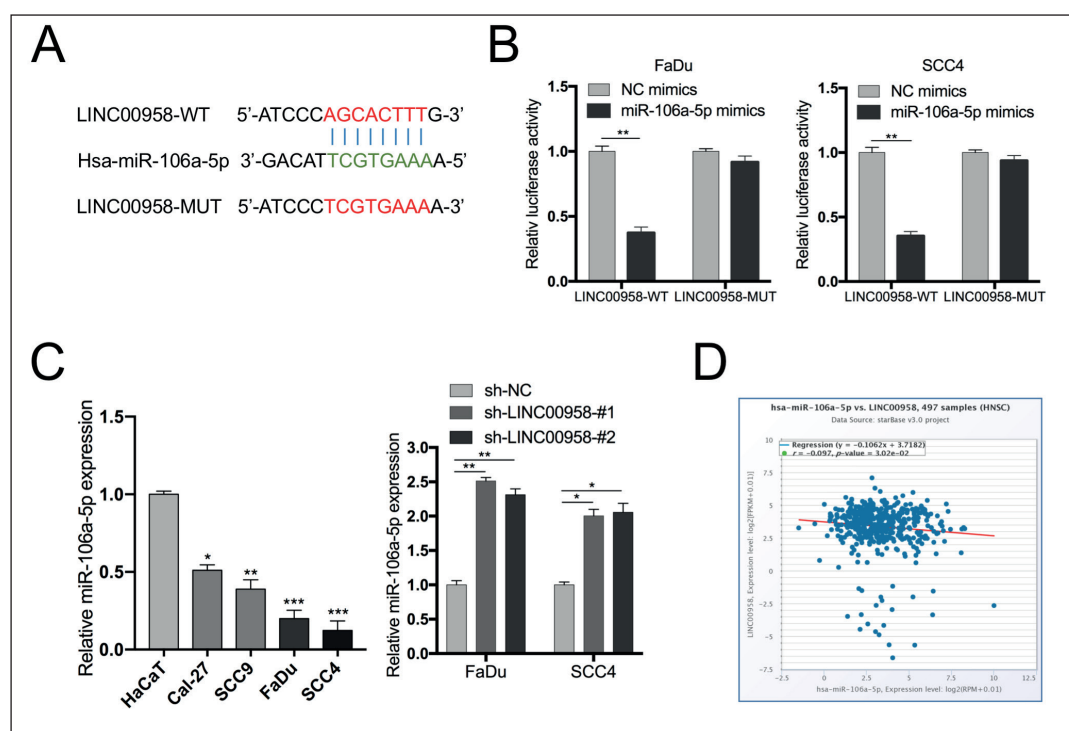


Figure 3. LINC00958 acted as sponge of miR-106a-5p in HNSCC cells. **A**, Prediction binding site of LINC00958 in miR-106a-5p 3'UTR. **B**, Dual luciferase reporter assay demonstrated the target relationship of LINC00958 with miR-106a-5p. **C**, Expression levels of miR-106a-5p were detected by qRT-PCR in HNSCC cells and LINC00958-silenced FaDu and SCC4 cells. **D**, The starbase dataset suggested that the expression level of LINC00958 and miR-106a-5p was negatively correlated in HNSCC tissue samples. * $p < 0.05$, ** $p < 0.01$, *** $p < 0.001$ compared to the control group.

Luciferase activity than those co-transfected by LINC00958 WT and NC mimics ($p < 0.05$), while the co-transfection with LINC00958 MUT and miR-106a-5p mimic did not significantly affect Luciferase activity of the cells, compared to the control. LINC00958 might bind to miR-106a-5p.

In addition, we found a negative correlation between the expression of miR-106a-5p and LINC00958 in HNSCC cells (Figure 3C; p all < 0.05). The StarBase database also revealed the same results in HNSCC tissues (Figure 3D; $p = 0.0302$). In summary, LINC00958 acted as a sponge of miR-106a-5p in HNSCC cells.

LINC00958 Knockdown Inhibited AKT/mTOR Signaling Pathway in HNSCC Cells

Reportedly, miR-106a-5p could regulate the phosphorylation level of AKT¹¹. Accumulating evidence indicates that the AKT/mTOR signaling pathway is strictly connected with the progression of HNSCC¹². Given the relationship between LINC00958 and miR-106a-5p, we investigated regulatory function of LINC00958 on AKT/mTOR signaling pathway in HNSCC. Western

blot analysis suggested that the knockdown of LINC00958 could remarkably suppress the expression of p-AKT and p-mTOR in FaDu cells and in SCC4 cells (Figure 4; p all < 0.01), revealing the inactivation of AKT/mTOR signaling pathway.

Oncogenic Function of LINC00958 Was Mediated by MiR-106a-5p

To study whether LINC00958 plays an oncogenic role by sponging miR-106a-5p, we co-transfected miR-106a-5p inhibitors into LINC00958 knockdown FaDu and SCC4 cells (sh-LINC00958-#2), and cells co-transfected by miR-NC were employed as controls. We found that the inhibitory effect of LINC00958 knockdown on growth and metastasis of HNSCC cells was reversed by miR-106a-5p inhibitor (Figure 5A-D; p all < 0.05). In addition, the results showed that the knockdown of LINC00958 evidently reduced the p-AKT and p-mTOR expression at protein level, and miR-106a-5p inhibitor partially rescued this reduction effect in HNSCC cells (Figure 5E; p all < 0.01). Collectively, these findings revealed that the oncogenic function of LINC00958 was mediated by miR-106a-5p.

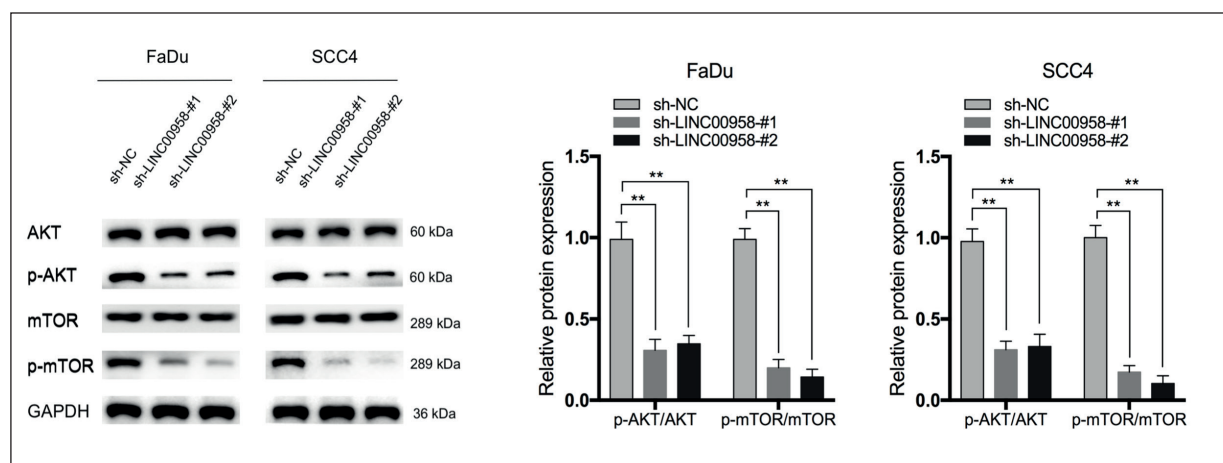


Figure 4. LINC00958 knockdown inhibited AKT/mTOR signaling pathway in HNSCC cells. Western blotting analysis revealed that the inhibition of LINC00958 in FaDu and SCC4 cells resulted in the down-regulation of p-AKT/AKT and p-mTOR/mTOR, revealing the inactivation of AKT/mTOR signaling pathway. ** $p < 0.01$.

Discussion

Despite advances in screening, diagnosis and multimodal treatments, the 5-year survival rate of HNSCC patients remains low¹³. This highlights the urgent need for new diagnostic and therapeutic target discovery. Recent studies have revealed that approximately 98% of human genome transcripts are non-coding RNAs (ncRNAs) with no protein-coding capacity. Over 68% genome transcripts are classified as lncRNAs¹⁴. LncRNAs have been confirmed to be involved in multiple cancer progression, including HNSCC¹⁵. In the present study, we used TCGA database to determine the significant upregulation of LINC00958 in HNSCC tissues. In addition, high LINC00958 level was correlated to unfavorable survival outcome of HNSCC patients. We, then, confirmed that LINC00958 was highly expressed in HNSCC cell lines by qRT-PCR. Loss-of-function experiments demonstrated that LINC00958 knockdown inhibited the proliferation, migration, and invasion of HNSCC *in vitro*. We adopted xenograft to verify that LINC00958 knockdown restrained the growth of HNSCC cells *in vivo*. MiRNAs are defined as ncRNAs with a length of 20-24 nucleotides¹⁶. Abundant studies have reported that miRNA sponge is the most commonly mechanism by which lncRNAs perform their post-transcriptional regulatory function¹⁷. Hence, we wondered whether LINC00958 could act as a miRNA sponge in HNSCC. We searched RNA 22 database and verified the binding between LINC00958 and miR-106a-5p using Dual-Lu-

ciferase reporter assay. Previous studies have demonstrated that many lncRNAs affect malignant phenotypes via sponging miR-106a-5p. In hepatocellular carcinoma, lncRNA TCL6 inhibits the proliferative, migratory, and invasive potentials by sponging miR-106a-5p¹¹. In ovarian cancer, lncRNA HOTAIRM1 suppresses cell proliferation and invasion by sponging miR-106a-5p¹⁸. In gastric cancer, lncRNA OIP5-AS1 promotes cell proliferation by targeting miR-106a-5p¹⁹. In nasopharyngeal carcinoma, lncRNA SMAD5-AS1 acts as a miR-106a-5p sponge to promote cell proliferation, migration, and invasion²⁰. However, few studies focused on the involvement of miR-106a-5p in HNSCC progression. Our study firstly showed that LINC00958 could act as a sponge of miR-106a-5p in HNSCC cells.

Dong et al²¹ suggested that miR-106a-5p could suppress tumorigenesis based on its inhibition on AKT/mTOR signaling pathway. The signaling network defined by PI3K, AKT and mTOR contributes to cancer-promoting processes such as growth, motility, metabolism, and proliferation²². Several studies^{23,24} have revealed that lncRNAs could promote the malignant progression in HNSCC via AKT/mTOR signaling pathway. Accordingly, we hypothesized that the regulatory mechanism of LINC00958 in HNSCC was probably associated with this signaling pathway. The results of our study indicated that LINC00958 downregulation could reduce the phosphorylation level of AKT and mTOR. The absence of miR-106a-5p could partially reverse this reduction effect of LINC00958 knockdown, suggesting

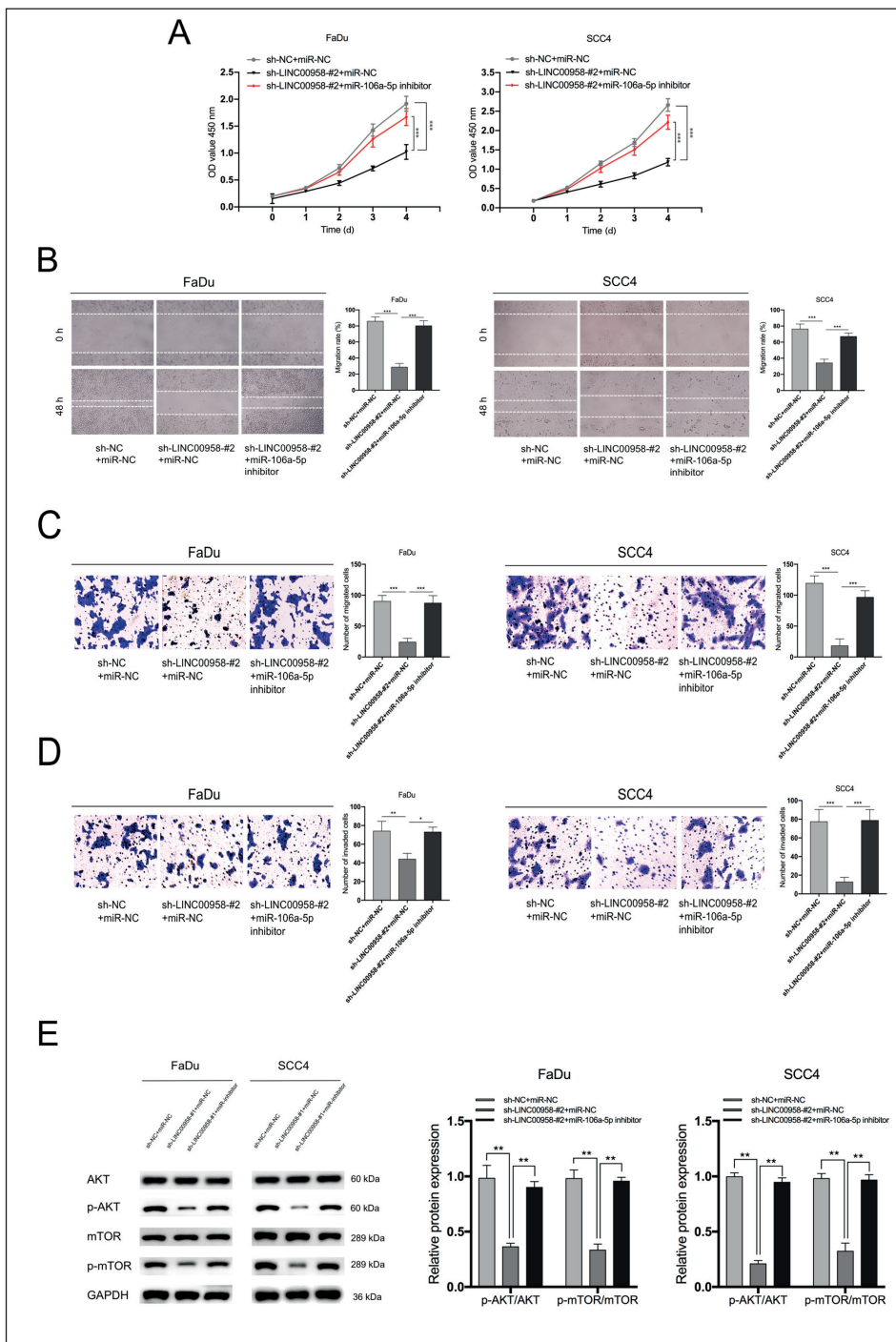


Figure 5. Oncogenic function of LINC00958 was mediated by miR-106a-5p. The inhibitory effect of LINC00958 knockdown on cell proliferation (**A**) migration (**B**) (magnification: 20×), invasion (**D**) (magnification: 100×), and AKT/mTOR signaling pathway (**E**) were significantly reversed by miR-106a-5p inhibitor. * $p < 0.05$, ** $p < 0.01$, *** $p < 0.001$ compared to the control group.

that regulatory function of LINC00958 on AKT/mTOR signaling pathway was depended on miR-106a-5p. In addition, miR-106a-5p knockdown could also rescue anti-tumor actions caused by the knockdown of LINC00958. All studies proved that LINC00958 might influence AKT/mTOR signaling pathway and malignant progression of HNSCC through targeting miR-106a-5p.

Conclusions

Taken together, these results demonstrated that lncRNA LINC00958 was upregulated in HNSCC and positively correlated with poor prognosis of patients. Silencing of LINC00958 had the ability to inhibit the proliferation, migration, and invasion of HNSCC. In addition, LINC00958 knock-

down could attenuate the aggressive progression and AKT/mTOR signaling pathway by targeting miR-106a-5p. These findings highlight the potential of LINC00958 as a promising prognostic biomarker and therapeutic target in HNSCC.

Funding Acknowledgments

This study was funded by grants from Beijing Municipal Natural Science Foundation [Grant No. 7184196], Beijing Municipal Administration of Hospitals' Ascent Plan [Grant No. DFL20180202], Capital Health Development Research Project [Grant No. S2018-2-2054], and Beijing Natural Science Foundation Program and Scientific Research Key Program of Beijing Municipal Commission of Education [Grant No. KZ201910025034].

Conflict of Interests

The authors declare that they have no competing interests or personal relationships that could have appeared to influence the work reported in this paper.

References

- LEEMANS CR, SNIJERS PJF, BRAKENHOFF RH. The molecular landscape of head and neck cancer. *Nat Rev Cancer* 2018; 18: 269-282.
- LYDIATT WM, PATEL SG, O'SULLIVAN B, BRANDWEIN MS, RIDGE JA, MIGLIACCI JC, LOOMIS AM, SHAH JP. Head and Neck cancers-major changes in the American Joint Committee on cancer eighth edition cancer staging manual. *CA Cancer J Clin* 2017; 67: 122-137.
- KOPP F, MENDELL JT. Functional classification and experimental dissection of long noncoding RNAs. *Cell* 2018; 172: 393-407.
- JIN S, YANG X, LI J, YANG W, MA H, ZHANG Z. p53-targeted lincRNA-p21 acts as a tumor suppressor by inhibiting JAK2/STAT3 signaling pathways in head and neck squamous cell carcinoma. *Mol Cancer* 2019; 18: 38.
- SEITZ AK, CHRISTENSEN LL, CHRISTENSEN E, FAARKROG K, OSTENFELD MS, HEDEGAARD J, NORDENTOFT I, NIELSEN MM, PALMFELDT J, THOMSON M, JENSEN MT, NAWROTH R, MAURER T, ORNTOFT TF, JENSEN JB, DAMGAARD CK, DYRSKJOT L. Profiling of long non-coding RNAs identifies LINC00958 and LINC01296 as candidate oncogenes in bladder cancer. *Sci Rep* 2017; 7: 395.
- SALMENA L, POLISENO L, TAY Y, KATS L, PANDOLFI PP. A ceRNA hypothesis: the Rosetta Stone of a hidden RNA language? *Cell* 2011; 146: 353-358.
- ZUO X, CHEN Z, GAO W, ZHANG Y, WANG J, WANG J, CAO M, CAI J, WU J, WANG X. M6A-mediated upregulation of LINC00958 increases lipogenesis and acts as a nanotherapeutic target in hepatocellular carcinoma. *J Hematol Oncol* 2020; 13: 5.
- ZHAO H, ZHENG GH, LI GC, XIN L, WANG YS, CHEN Y, ZHENG XM. Long noncoding RNA LINC00958 regulates cell sensitivity to radiotherapy through RRM2 by binding to microRNA-5095 in cervical cancer. *J Cell Physiol* 2019; 234: 23349-23359.
- YANG L, LI L, ZHOU Z, LIU Y, SUN J, ZHANG X, PAN H, LIU S. SP1 induced long non-coding RNA LINC00958 overexpression facilitate cell proliferation, migration and invasion in lung adenocarcinoma via mediating miR-625-5p/CPSF7 axis. *Cancer Cell Int* 2020; 20: 24.
- CHEN S, CHEN JZ, ZHANG JQ, CHEN HX, QIU FN, YAN ML, TIAN YF, PENG CH, SHEN BY, CHEN YL, WANG YD. Silencing of long noncoding RNA LINC00958 prevents tumor initiation of pancreatic cancer by acting as a sponge of microRNA-330-5p to down-regulate PAX8. *Cancer Lett* 2019; 446: 49-61.
- LUO LH, JIN M, WANG LQ, XU GJ, LIN ZY, YU DD, YANG SL, RAN RZ, WU G, ZHANG T. Long noncoding RNA TCL6 binds to miR-106a-5p to regulate hepatocellular carcinoma cells through PI3K/AKT signaling pathway. *J Cell Physiol* 2020;
- MARQUARD FE, JUCKER M. PI3K/AKT/mTOR signaling as a molecular target in head and neck cancer. *Biochem Pharmacol* 2020; 172: 113729.
- GATTA G, BOTTA L, SANCHEZ MJ, ANDERSON LA, PIERANNUNZIO D, LICITRA L. Prognoses and improvement for head and neck cancers diagnosed in Europe in early 2000s: The EUROCARE-5 population-based study. *Eur J Cancer* 2015; 51: 2130-2143.
- IYER MK, NIKNAFS YS, MALIK R, SINGHAL U, SAHU A, HOSONO Y, BARRETTE TR, PRENSNER JR, EVANS JR, ZHAO S, POLIAKOV A, CAO X, DHANASEKARAN SM, WU YM, ROBINSON DR, BEER DG, FENG FY, IYER HK, CHINNAIYAN AM. The landscape of long noncoding RNAs in the human transcriptome. *Nat Genet* 2015; 47: 199-208.
- MA H, CHANG H, YANG W, LU Y, HU J, JIN S. A novel IFN α -induced long noncoding RNA negatively regulates immunosuppression by interrupting H3K27 acetylation in head and neck squamous cell carcinoma. *Mol Cancer* 2020; 19: 4.
- D'ANGELO B, BENEDETTI E, CIMINI A, GIORDANO A. MicroRNAs: A Puzzling Tool in Cancer Diagnostics and Therapy. *Anticancer Res* 2016; 36: 5571-5575.
- THOMSON DW, DINGER ME. Endogenous microRNA sponges: evidence and controversy. *Nat Rev Genet* 2016; 17: 272-283.
- CHAO H, ZHANG M, HOU H, ZHANG Z, LI N. HO-TAIRM1 suppresses cell proliferation and invasion in ovarian cancer through facilitating ARHGAP24 expression by sponging miR-106a-5p. *Life Sci* 2020; 243: 117296.
- WANG LW, LI XB, LIU Z, ZHAO LH, WANG Y, YUE L. Long non-coding RNA OIP5-AS1 promotes proliferation of gastric cancer cells by targeting miR-641. *Eur Rev Med Pharmacol Sci* 2019; 23: 10776-10784.
- ZHENG YJ, ZHAO JY, LIANG TS, WANG P, WANG J, YANG DK, LIU ZS. Long noncoding RNA SMAD5-AS1 acts as a microRNA-106a-5p sponge to promote epithelial mesenchymal transition in nasopharyngeal carcinoma. *FASEB J* 2019; 33: 12915-12928.

- 21) DONG S, ZHANG X, LIU D. Overexpression of long noncoding RNA GAS5 suppresses tumorigenesis and development of gastric cancer by sponging miR-106a-5p through the Akt/mTOR pathway. *Biol Open* 2019; 8:
- 22) HANAHAN D, WEINBERG RA. Hallmarks of cancer: the next generation. *Cell* 2011; 144: 646-674.
- 23) YANG Y, CHEN D, LIU H, YANG K. Increased expression of lncRNA CASC9 promotes tumor progression by suppressing autophagy-mediated cell apoptosis via the AKT/mTOR pathway in oral squamous cell carcinoma. *Cell Death Dis* 2019; 10: 41.
- 24) ZHAO R, TIAN L, ZHAO B, SUN Y, CAO J, CHEN K, LI F, LI M, SHANG D, LIU M. FADS1 promotes the progression of laryngeal squamous cell carcinoma through activating AKT/mTOR signaling. *Cell Death Dis* 2020; 11: 272.